International Journal of Design & Nature and Ecodynamics
Vol. 19, No. 6, December, 2024, pp. 2117-2126
Journal homepage: http://iieta.org/journals/ijdne

The Gavrilovic Model to Estimate the Volume of Water Erosion in Al-Ratka Valley Basin

Awrad Imad Shehab*, Ahmed Flayyih Fayyadh

Department of Geography, College of Education for Humanities, University of Anbar, Anbar 31001, Iraq

Corresponding Author Email: awrad.e.sh@uoanbar.edu.iq

https://doi.org/10.18280/ijdne.190628

Received: 16 September 2024
Revised: 12 November 2024
Accepted: 20 November 2024
Available online: 27 December 2024

Keywords:
Ratka Valley basin, water erosion, Gavrilovic model

ABSTRACT

The study of water erosion is of great importance in order to know the degree of surface sensitivity because it represents a basic step for environmental assessment due to its reflection on the dominance of land types and uses, especially in arid and semi-arid regions that suffer from a fragile ecosystem due to the prevalence of drought and climate extremes. The application of the potential erosion method, or the so-called Potential Method Erosion model, was relied upon, as it represents one of the experimental and semi-quantitative methods through which the amount of sedimentary revenue can be estimated as well as the degree and severity of erosion. The research aims to employ geographic information systems techniques to estimate erosion according to the Gavrilovic equation, as this model gives two types of erosion. The first is known as potential specific erosion (Z), in which all data are used except climatic factors. The second is known as final soil losses (W). It uses all data, including climatic factors. In building the erosion model (EPM), we relied on remote sensing data represented by satellite data (Landsat 8), the digital elevation model (DEM), and soil and rainfall data, because of their fundamental role in the activity of erosion processes. Among the most important results of using this model were divided The study area is divided into five erosion levels: "Among the most important results of using this model, the study area was divided into five levels of erosion: very low erosion, with an area of (514) km², accounting for (7.2%); low erosion, with an area of (529) km² and a percentage of (7.4%); moderate erosion, with an area of (2631) km², accounting for (36.9%); severe erosion, with an area of (2102) km² and a percentage of (29.5%); and very severe erosion, with an area of (1358) km², accounting for (19%)".

1. INTRODUCTION

Water erosion plays a crucial role in hydrogeomorphological research due to its significant impact on shaping the Earth's surface features. In the study area, these features may not solely result from the current climate conditions but rather trace back to a wetter period in the past, characterized by heavy rains that contributed to soil breakdown and its subsequent transport by water to different areas where it got deposited.

In the present era, although rainfall is infrequent, it occurs in the form of intense showers that facilitate the erosion process. However, the extent of erosion is dependent on several factors, including the amount and type of precipitation, the nature of the terrain, slope gradient, and vegetation density [1].

The quality of the rocks also plays a significant role in the erosion process; fragile rocks are more susceptible to erosion compared to hard ones, influenced by the materials binding the grains. Soluble materials increase the likelihood of erosion. Vegetation cover is another critical factor, as it helps slow down water flow, allowing more water to infiltrate the earth's surface. Additionally, the roots of vegetation help in soil retention. However, the study area is characterized by a lack of vegetation cover, with desert soil predominating [2]. These factors contribute to variations in erosion processes across different regions within the study area. Recognizing that erosion is a global phenomenon, various mathematical models have been developed to quantify soil loss. One such model employed in this study is the Gavrilovic EPM model. The Gavrilovic model, attributed to Slobodan Gavrilovic, was developed in collaboration with researchers at the Institute of Water Resources in Yugoslavia over a period spanning from 1952 to 1976, consisting of three stages [3]. This model has since become the standard tool for assessing water erosion extent and sedimentation in European countries, including the Eastern Region, over recent decades. Stefanovic and colleagues recognize its widespread adoption in the field of water resources management for evaluating surface erosion [4]. The Gavrilovic model operates on two fundamental aspects. The first aspect involves the incorporation of specific indicators into the model. These indicators include variables such as "T", "H", "Xa", "Q", "Y", and "Ja". These indicators are entered with their actual values, without being subjected to mathematical transformations, in order to assess the levels of water erosion and their corresponding environmental risks within the region [5]. The second aspect revolves around the utilization of membership functions for these indicators,

assigning values ranging between 0 and 1. Subsequently, the Gavrilovic equation is applied to these indicators, resulting in output values that also fall within the range of 0 to 1. The primary purpose of employing this model is to categorize the intensity of erosion and to determine the associated degree of environmental risk, particularly regarding soil erosion [6].

1.1 Research questions

1- To what extent does water erosion affect Ratka Valley basin?
2- Is it feasible to develop models that accurately replicate real-world conditions using a geoinformation environment to assess erosion levels in Ratka Valley basin and its associated sub-basins?
3- Can the Gavrilovic model be regarded as a reliable scientific advisory tool for the study area's basins?

1.2 Study hypotheses

1- The extent of water erosion in Ratka Valley basin exhibits varying degrees, ranging from very weak to severe, depending on the spatial characteristics of the basins. Notably, climate factors, particularly precipitation, play a significant role in driving the erosion process. Other influential factors include the geological structure, terrain, slope, soil composition, and natural vegetation.
2- It is possible to develop models that accurately replicate real-world conditions using a geoinformation environment to assess the extent of erosion in Ratka Valley basin and its associated sub-basins.
3- The Gavrilovic model can be considered a scientifically sound advisory tool for evaluating the basins within the study area.

2. STUDY AREA LOCATION

The study area is situated in the western part of Iraq, specifically within Anbar Governorate, as indicated on Figure 1. This basin represents a natural geographic unit covering an area of approximately 7,134 square kilometers. Consequently, the region is bounded by two latitudes, ranging from (32°55'1"N 34°17'38.4"N), to the north, and two longitudes, extending from (39°36'18"E 40°46'44"E) to the east [7].

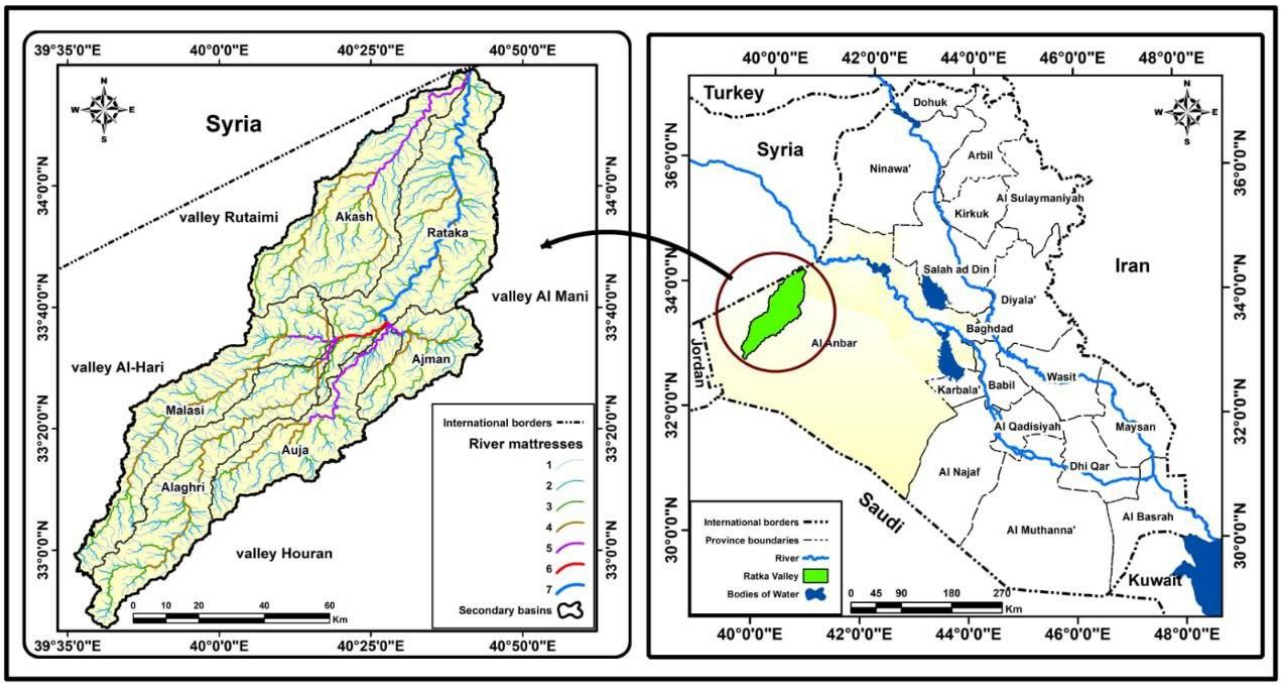

Figure 1. Location of the study area in Iraq
Source: Based on the Republic of Iraq, Ministry of Industry and Minerals, General Establishment for Geological Survey and Mineral Investigation, Administrative Map of Iraq, year 2000, scale 1:250000, and Arc Gis 10.8 program.

2.1 Mechanism for constructing the Gavrilovic erosion model (EPM)

The study of water erosion holds significant importance as it allows us to assess surface susceptibility, which is a fundamental step in environmental evaluation, impacting land types and usage. In this regard, we have employed the Potential Method Erosion model, also known as the Potential Erosion method. This model is considered one of the experimental and semi-quantitative approaches that enable the estimation of sedimentary income and the determination of erosion severity and extent [8].

2.1.1 Model building data

Landsat 8, the eighth installment in the Landsat program, is an American satellite that was successfully launched on February 11, 2013. This advanced satellite has the capability to capture detailed maps of Earth's surface within a 16-day timeframe, gathering crucial data, particularly pertaining to forests, water bodies, and agricultural regions. This visualization encompasses 11 distinct spectral bands, each tailored to a specific purpose, as detailed in Table 1.

This data type was utilized in the calculation of the (Xa) coefficient, which was derived from a combination of channels within the range (2, 3, 4, 5, 6, 7, 8). This combination process resulted in a colored visual representation that facilitates the

identification of various types of plant cover, a critical component for determining this coefficient.

Table 1. Data transmission for Landsat 8 and its applications

Clarity Degree	Wave Length	Ranges	
30	0.43-0.45	Band 1-Coastal Aerosol	Landsat 8 Operational Land Imager (OLI) and Thermal Infrared Sensor (TIRS), February 11, 2013
30	0.45-0.51	Band 2–Blue	
30	0.53-0.59	Band 3–Green	
30	0.64-0.67	Band 4–Red	
30	0.85-0.88	Band 5-Near Infrared (Vegetation)	
30	1.57-1.65	Band 6-Shortwave Infrared (SWIR) 1	
30	2.11-2.29	Band 7-Shortwave Infrared (SWIR) 2	
15	0.50-0.68	Band 8–Panchromatic	
30	1.36-1.38	Band 9-Cirrus (Clouds)	
100	10.60-11.19	Band 10-Thermal Infrared (TIRS) 1	
100	11.50-12.51	Band 11-Thermal Infrared (TIRS) 2	

Another valuable aspect of these visualizations is the ability to derive temperature data, primarily from zones (10, 11). This involves applying a specific mathematical algorithm, which we will elaborate on later. Regarding the assessment of current erosion, the fourth band is employed, focusing on the maximum radiation value as a key indicator [9].

2.2 Digital elevation model (DEM)

It is essentially a data file containing a series of elevation points distributed across the Earth's surface. Vertically, these points are associated with elevation values (Z) relative to sea level or a specific reference point, while horizontally, they are linked to known grid values (X, Y) corresponding to the fundamentals of a map [10]. To acquire this type of visualization, we turned to the Earth Data website of the US Geological Survey (USGS), specifically using data from the ALOS-PALSAR satellite. This source provides data with a remarkable level of accuracy, down to (12.5) meters. The digital elevation model played a crucial role in our work, particularly in deriving the slope index (Ja), a pivotal component in the construction of a water erosion risk map.

2.3 Soil data

The distribution of soil in the region is primarily influenced by both climate and surface erosion patterns, and as such, it aligns with the classification system provided by the Food and Agriculture Organization (FAO), recognized as one of the most contemporary soil classifications worldwide [11].

2.4 Precipitation data

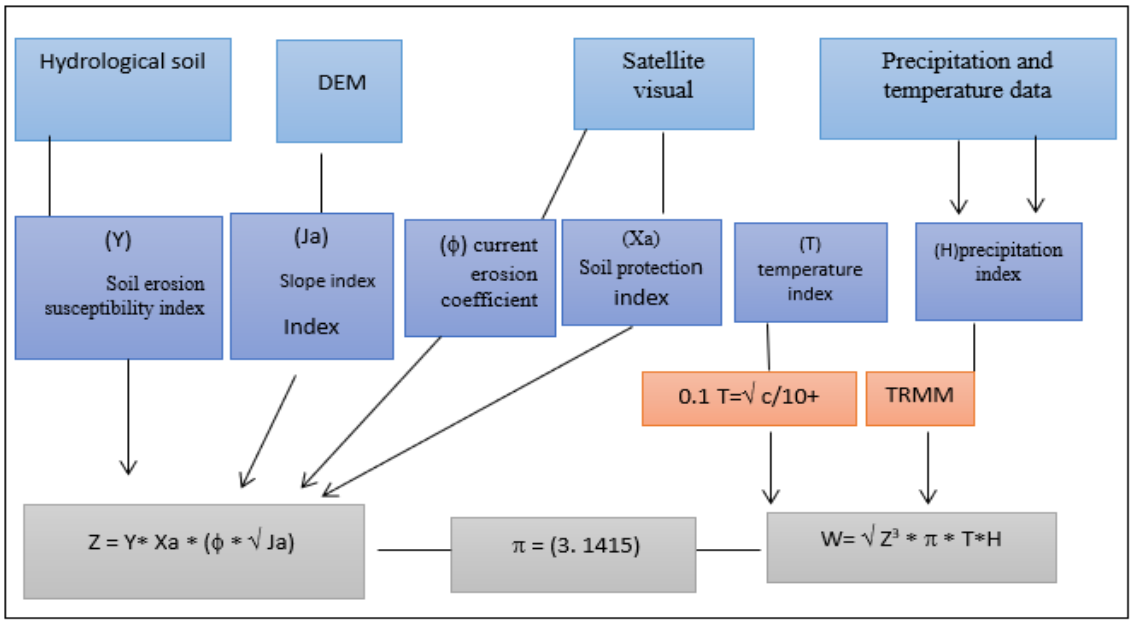

Figure 2. Steeps of the methodology

Rainfall plays a pivotal role in driving water erosion within the study area. It initiates the erosion process, starting with raindrops and leading to surface runoff and eventually drainage channels. Intense rain showers are especially influential in washing away substantial amounts of soil, particularly in areas characterized by steep slopes and a lack of vegetation cover. The Tropical Rainfall Measuring Mission (TRMM) model, a collaborative project between NASA and the Japan Aerospace Exploration Agency, served as a valuable resource for precipitation data. The TRMM model operated for approximately 17 years, temporarily ceasing in April 2015 before re-entering Earth's atmosphere in June 2015. To this day, the model continues to monitor and study tropical rainfall [12].

2.5 Application of data to water erosion indicators

To estimate erosion, Geographic Information Systems (GIS) techniques were employed in accordance with the Gavrilovic-Lovec equation. This model provides two types of erosion indicators: potential specific erosion (Z), which uses all available data except for climatic factors, and final soil losses (W), which incorporates all data, including climatic factors. Figure 2 illustrates the workflow of this model [13, 14].

3. TEMPERATURE INDEX (T)

Temperature plays a fundamental role in the initiation of mechanical weathering processes, directly affecting the fragmentation, flaking, breaking, and dispersion of rock grains. This impact is particularly pronounced when there are significant daily temperature fluctuations. Additionally, temperature levels influence the moisture content of rocks and sediments, contributing to processes like decomposition, oxidation, and hydration of rock minerals. Gavrilovic determined the temperature factor through a dedicated equation that relies on the annual average temperature as the key variable for its calculation, as expressed in the following equation (Figure 3) [13].

$$T = \sqrt{(c/10 + 0.01)}$$

where, c represents the average annual temperature.

To obtain climate data for calculating T, information from weather stations in Al-Qaim, Al-Nukhayb, Al-Rutba, and Deir ez-Zor was utilized. These data sets were processed using the ArcGIS 10.8 program, as shown in Table 2 and Figure 4.

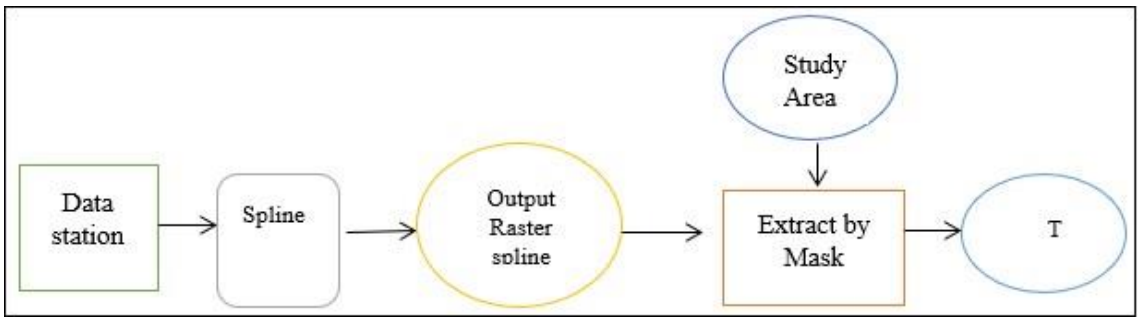

Figure 3. Illustration of the construction of T indicator model

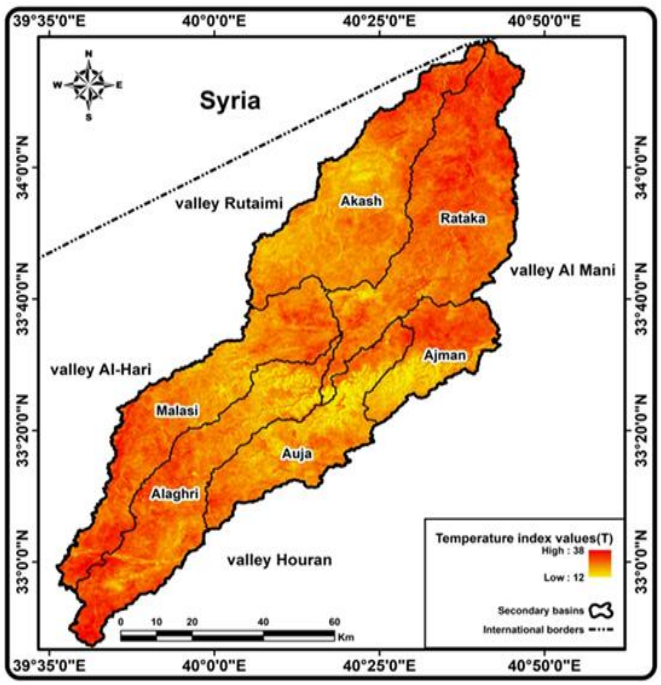

Figure 4. The T index for the study area basins

Table 2. Monthly and annual average temperatures (°C) at the stations (Rutbah, Al-Nukhayb, Al-Qaim, Deir ez-Zor) for the period (1990-2020)

Months	Rutbah	Al-Nukhayb	Al-Qaim	Deir ez-Zor
January	6.9	9.8	8.8	7.4
February	9.8	12.5	10.2	9.4
March	13.6	15.7	14.2	13.1
April	20.9	23.5	22.9	19.7
May	23.6	28.1	26.1	25.3
June	28.8	32.9	33.1	30.3
July	31.9	35.8	34.2	34.6
August	31.7	34.7	33.9	34.4
September	28	30.7	29.6	33.1
October	20.8	25.7	24.9	26.8
November	14.9	16.9	14.9	16.7
December	9.4	12.6	12.5	9.4
Annual rate	20.02	24.2	22.1	21.7
Thermal range	25	26	25.4	27.2

4. PRECIPITATION INDEX (H)

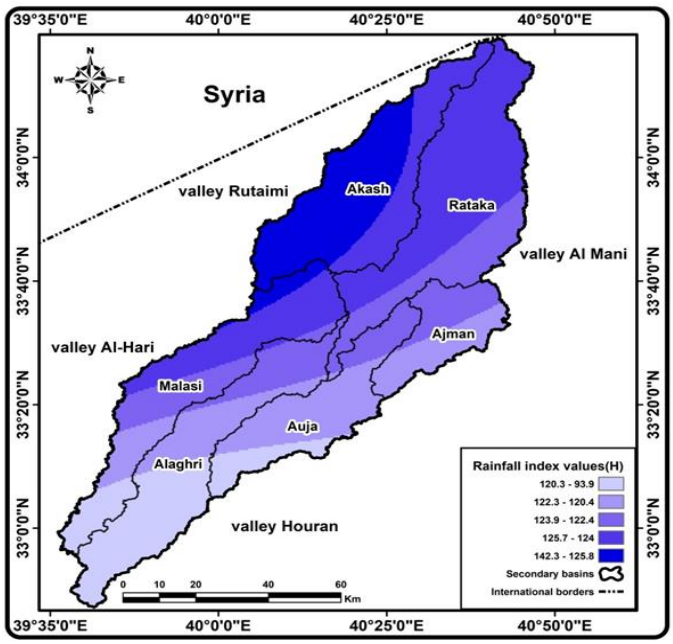

Figure 5. Rainfall index H according to TRMM

Rainfall is a critical factor influencing the erosion process. To calculate the precipitation index (H), climate data was collected based on the Tropical Rainfall Measuring Mission (TRMM) model. This model is the result of a joint space mission between NASA and the Japan Aerospace Exploration Agency (JAXA), providing climate data on rainfall from 1990

to 2020. In this model, monthly precipitation rates over a 20-year period were considered, and the study area was extracted from this model [15]. A specialized tool was then designed to delineate the study area, and the values of the grid cells were converted into point values, resembling rainfall measurement locations. Subsequently, these values were reconverted into grid cell values. This process is depicted in Figure 5 and Figure 6 [16].

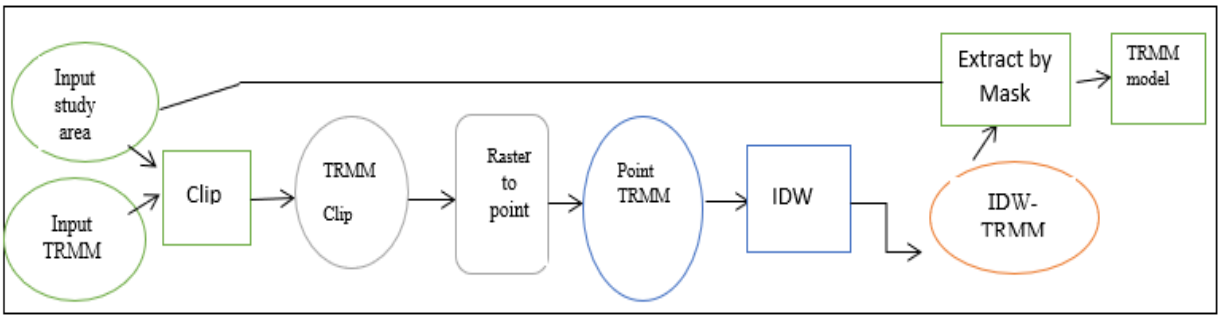

Figure 6. Building an H index model

5. THE SOIL EROSION SUSCEPTIBILITY INDEX (Y)

Y is defined as the impact of soil properties on soil loss during precipitation and its sensitivity to water erosion. It is influenced by geological properties, soil characteristics, and land use [17]. To calculate the soil erosion susceptibility factor, data from the geological map and the hydrological soil map of the study area were utilized. While there are specific equations for deriving the soil erosion susceptibility factor based on laboratory analyses, these were not available for this study. Instead, the researcher relied on the hardness of rocks and soil texture, as outlined in Table 3, Figures 7 and 8 [18].

Table 3. The different resistance types of soil and rocks based on the value of the Y index

Soil Erosion Potential (Y)	Km^2	Percentage
Very weak	3691	51.7
Weak	2851	40
Medium	423	5.9
Strong	127	1.8
Very strong	42	0.6
Total summation	Km^2	100

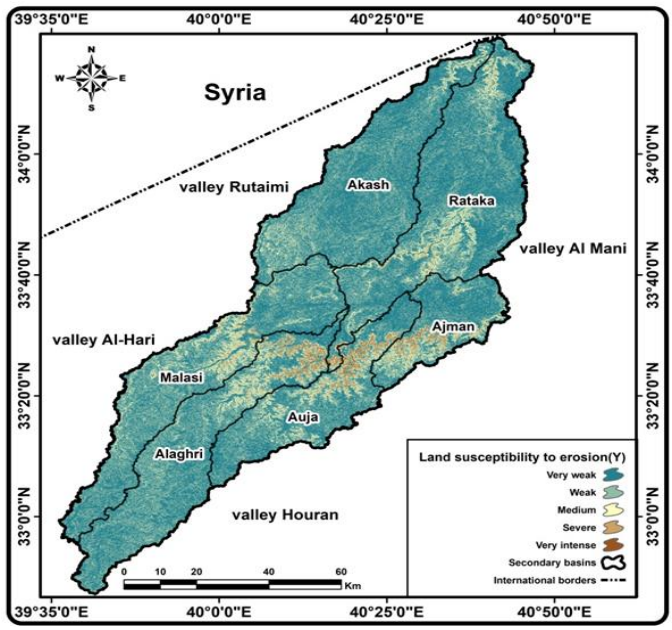

Figure 7. The soil erosion susceptibility index (Y) across the study area

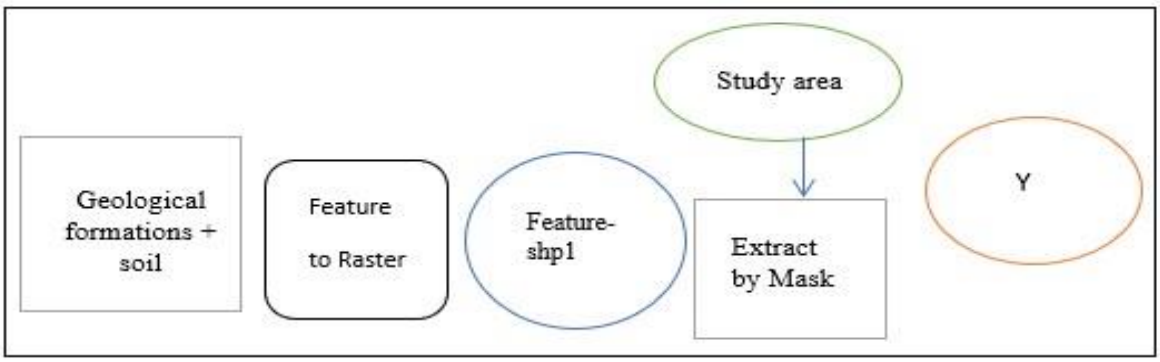

Figure 8. Soil erosion susceptibility index Y

The soil erosion susceptibility index was categorized into five classes according to the Gavrilovic model, as depicted in Figure 7 and detailed in Table 3 [19].

1. The first category corresponds to "very weak," covering an area of 3,691 km^2, accounting for 51.7% of the total area. This category is scattered across the study area basins.
2. The second category represents "weak," with an area of 2,851 km^2, constituting 40% of the total area. This category prevails in most parts of the study area.
3. The third category signifies "medium," covering an area of 423 km^2, equivalent to 5.9% of the total area.

4. The fourth category denotes "severe," encompassing an area of 127 km^2, making up 1.8% of the total area.
5. The fifth category signifies "very severe," with an area of 42 km^2, accounting for 0.6% of the total area.

The Slope Index (Ja): is influenced by various factors, leading to variations in slope characteristics. The study area is categorized as having predominantly flat slopes, as illustrated in Figure 9 and Figure 10 [20].

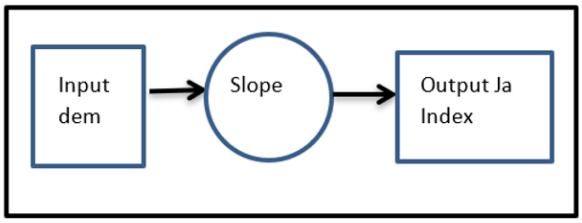

Figure 9. Building JA indicator model

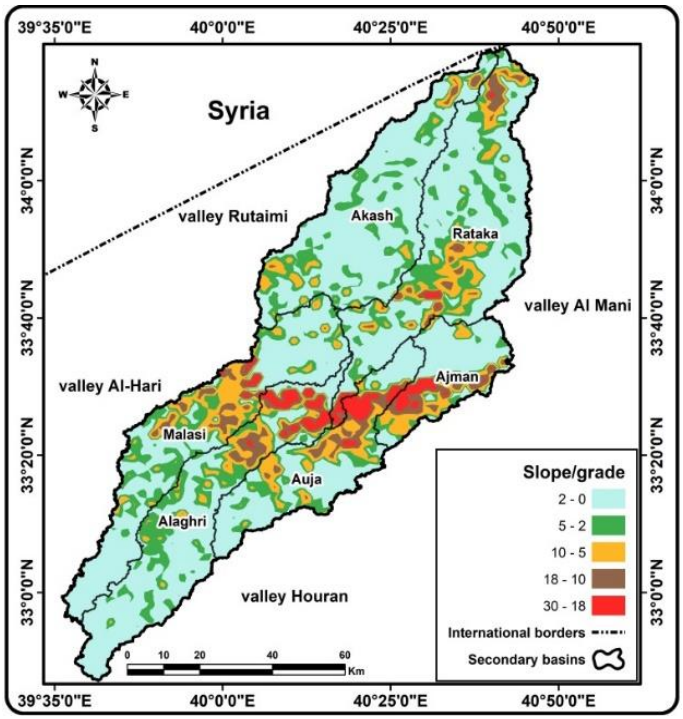

Figure 10. Regression levels for the study area according to young's classification

The information for this classification was derived from a Digital Elevation Model (DEM) with a resolution of (30×30) meters and a surface map of Anbar Governorate at a scale of 1:100,000. These data were processed using ArcGIS 10 software.

6. THE SOIL PROTECTION INDEX (XA)

Is defined as the levels of vegetation density that contribute to soil stabilization, reduction of flow velocity, improved water permeability, and erosion reduction [21]. It is directly proportional to vegetation density. A classification process was performed on a Landsat 8 satellite image captured on 7/3/2022 to determine the types of vegetation cover based on Xa values. These values were then classified into five categories, as outlined in Table 4 and Figure 11.

Accordingly, the study area's basins were classified into the following categories:

1. The first category corresponds to "very weak," covering an area of 1,258 km^2, representing 17.6% of the total area. This category is dispersed across the study area basins.
2. The second category represents "weak," with an area of 1,069 km^2, constituting 15% of the total area. This category dominates most of the study area.
3. The third category corresponds to "medium," covering an area of 1,570 km^2 and representing 22% of the total area. This category is distributed across the entire study area.
4. The fourth category corresponds to "severe" erosion, covering an area of 1,686 km^2 and representing 23.6% of the total area.
5. The fifth category represents "very severe" erosion, with an area of 1,551 km^2, accounting for 21.7% of the total area. This category is mainly concentrated in the central parts of the study area [22].

Table 4. The soil protection index Xa

Soil Protection Index (Xa)	Km^2	Percentage
Very weak	1258	17.6
Weak	1069	15
Medium	1570	22
Strong	1686	23.6
Very strong	1551	21.7
Total summation	7134	100

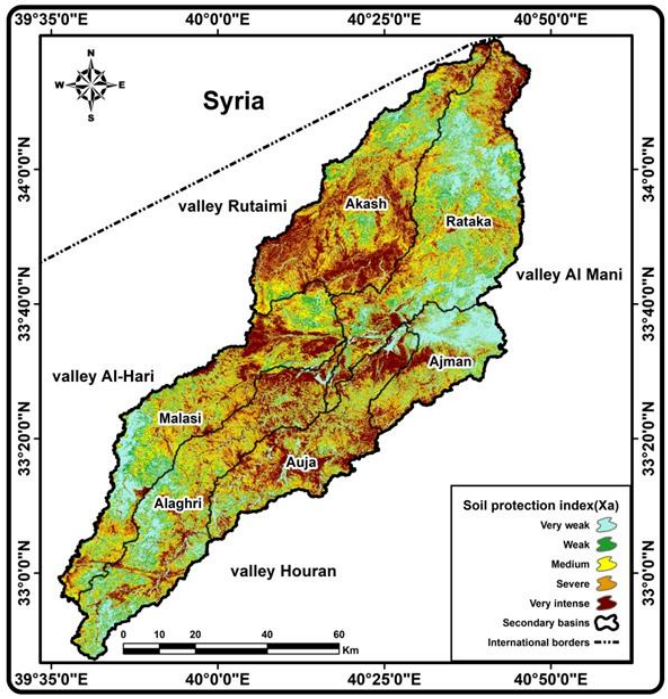

Figure 11. A visual representation of this index

6.1 The current erosion coefficient ∅

The values of the current erosion index vary with the sizes of the water basins, and the current erosion index was obtained through the equation formulated by study [23]. To calculate this index, where reliance was placed on Landsat 8 satellite visualization captured on 3/7/2022. According to the following equation:

$$\varnothing = \sqrt{Tm3/Qmax}$$

This equation is based on the square root of the third band (Tm3) divided by the maximum radiation value in Landsat 5. When the third band in the Landsat 5 satellite is compared with the Landsat 8 satellite, from the wavelength aspect we notice that the third band in the Landsat 5 satellite corresponds to Band 4 on the Landsat 8 satellite, so it is possible to modify the equation formula as follows [24]:

$$\varnothing=\sqrt{(band4(0.64-0.69)/Qmax)}$$

From the results of this equation, the extents of erosion are determined, as shown in Table 5 and Figure 12, according to the percentage of radiation, as the percentage of radiation increases steadily with the increase in the intensity of erosion.

Table 5. The values of the current erosion coefficient index (∅)

Evolution Current Erosion	Km²	Percentage
Very weak	1363	19.1
Weak	1494	20.9
Medium	1382	19.4
Strong	1463	20.5
Very strong	1432	20.1
Total summation	7134	100

Source: The data was processed by the researcher using the ArcGIS 10.8 program.

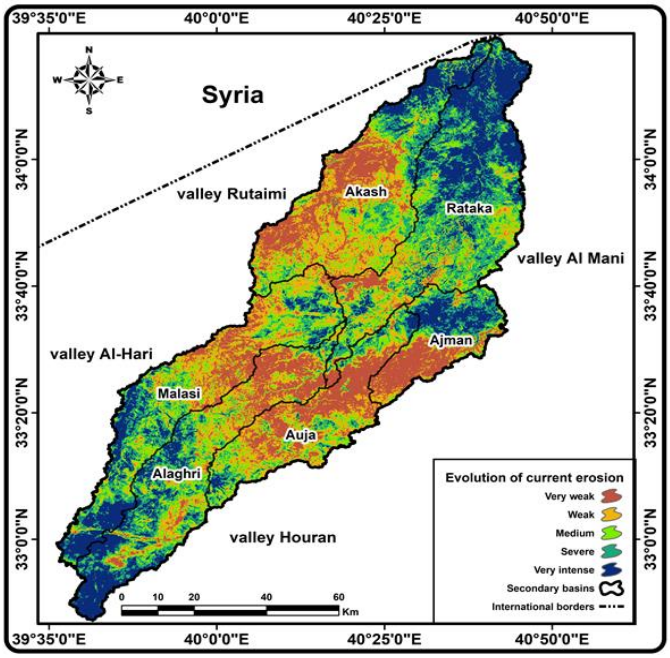

Figure 12. A visual representation of the current erosion coefficient index (∅) in the Gavrilovic model

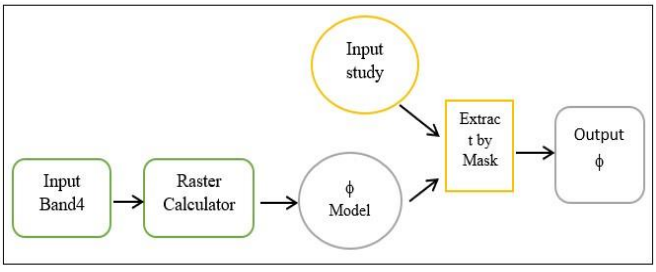

Figure 13. Illustration of the process of building the indicator model (∅)

A model for this parameter was created using the ArcGIS 10.8 program. Its inputs include the fourth band in Landsat 8 and the maximum radiation percentage for the band, as illustrated in Figure 13 [25].

6.2 Designing the Gavrilovic model (EPM)

After extracting the indicators mentioned above by applying their respective equations and automated processing, both quantitative and qualitative aspects of water erosion were determined. This model involves a series of transformational operations to obtain the final version of the model. Here are the details [26].

6.3 Specific erosion coefficient Z

This is a composite model that combines the Xa factor with the Y factor and multiplies them by the current erosion factor. Its values range between 1 and 0, and it can exceed 1 in cases of very severe erosion. Gavrilovic categorized the results into five qualitative classes, as shown in Table 6 and Figure 14 [27].

Table 6. Classifications and values of the Z index for specific erosion

Types Erosion	Qualitative Value
Very weak	0.19-0.01
Weak	0.40-0.20
Medium	0.41-0.80
strong	1.0-0.81
Very strong	1.1 and more

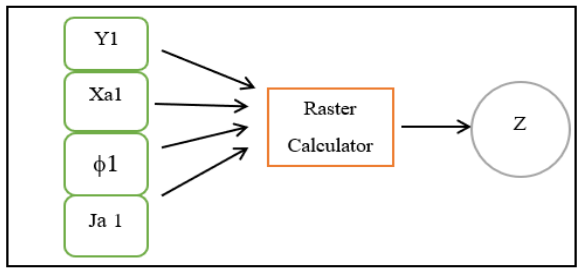

Figure 14. Illustration of the process of building the Z index model

Table 7. An overview of the types and areas of Z values for specific erosion

Types Erosion	Qualitative Value	Km²	Percentage
Very weak	0.01-1.19	514	7.2
Weak	0.20-0.40	529	7.4
Medium	0.41-0.80	2631	36.9
Strong	0.81-1.0	2102	29.5
Very strong	1.1 and more	1358	19
Qualitative value		7134	100

Based on Table 7 and Figure 15, the region can be divided into five categories:

1. Very Weak Erosion: This type covers an area of 514 km², accounting for 7.2% of the region. It is predominant in isolated areas within the study area's basins.
2- Weak Erosion: Covering an area of 529 km², this type represents 7.4% of the region and is prevalent in separate parts of the area.
3- Moderate Erosion: This type, with an area of 2,631 km²,

constitutes 36.9% of the region. It is the dominant type in most of the study area and occupies the largest portion of the basins [28].

4- Severe Erosion: Covering an area of 2,102 km^2, this category accounts for 29.5% of the region.

5- Very Severe Erosion (Class V): This category encompasses an area of 1,358 km^2, making up 19% of the region, primarily located in the northern and central parts of the study area [29].

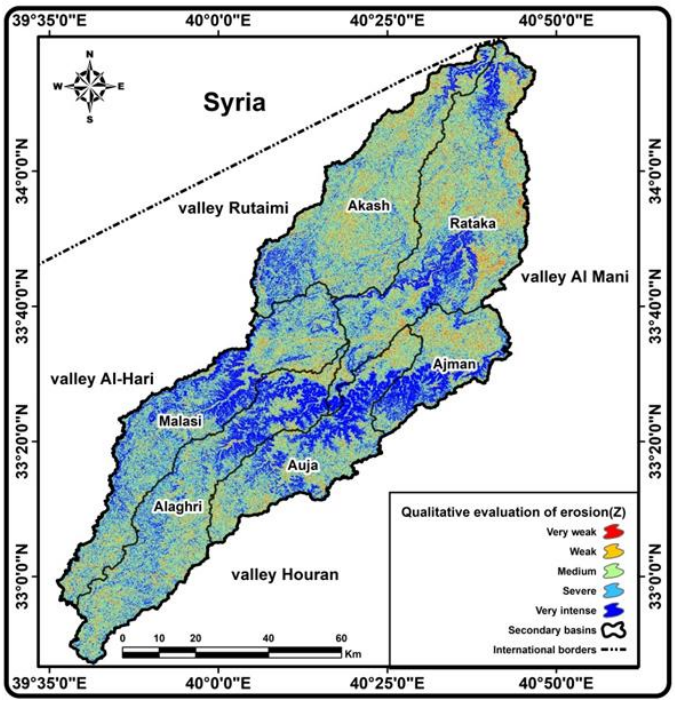

Figure 15. Visualizes the Z index for specific erosion across the study area

6.3 Quantitative erosion coefficient W

The final quantitative erosion coefficient integrates all indicators that affect erosion processes within the study area. It combines the qualitative erosion coefficient (Z) with the two climate factors (H, T) using the equation shown in Figure 16. Gavrilovic classified this factor into six categories, as detailed in Table 8 [30].

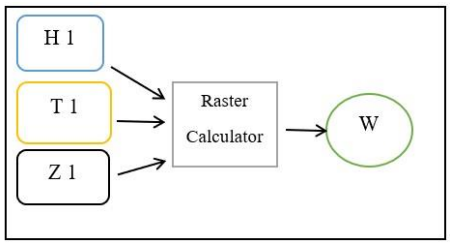

Figure 16. Building the W indicator model

Through Table 9 and Figure 17, erosion risks can be divided based on the amount of erosion within the basins of the study area into the following:

1. The First Type, Very Weak Erosion: The area of this type is 1116 km^2 and the percentage is 15.6%, and it prevails in separate parts of the region.
2. The Second Type, Weak Erosion: The area of this type is 1342 km^2 and the percentage is 18.8%, and it prevails in separate parts of the region.
3. The Third Type, Moderate Erosion: The area of this type is 2201 km^2 and the percentage is 30.9%, and it occupies the largest area of the basins of the study area. This type represents the dominant type in the region.
4. The Fourth Type, Severe Erosion: The area of this category is 1340 km^2 and the percentage is 18.8%.
5. The Fifth Type, Very Severe Erosion: The area of this class is 1135 km^2 and the rate is 15.9%. This class prevails in the central parts of the study area [31].

Table 8. Types and values of the W index for quantitative erosion

Types Erosion	Erosion Quantities/m^3/km^2/Year
Very weak	Less than 50
Weak	500-51
Medium	1500-501
strong	5000-1501
Very strong	20000-5001
Catastrophic	And more 20001

Table 9. Categories, area, and percentages of the W indicator within the basins of the study area

Quantitative Assessment Factor for Erosion (w)	Km^2	Percentage
Very weak	1116	15.6
Weak	1342	18.8
Medium	2201	30.9
Strong	1340	18.8
Very strong	1135	15.9
Qualitative value	7134	100

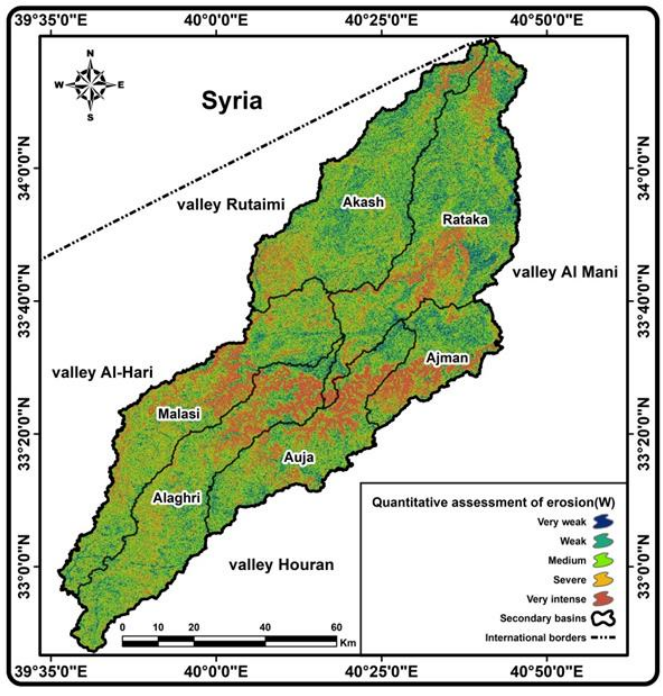

Figure 17. W index for quantitative erosion of the basins of the study area

7. CONCLUSIONS

1. The study concludes through the study that natural factors have an influential role in water erosion, which

are (precipitation, slope, soil susceptibility to erosion, and temperatures).
2. The EPM model is an appropriate model that simulates the reality of the geoinformation environment to detect the extent of erosion in the Wadi Ratka basin and its secondary basins.
3. The nature of the climate in the study area has a fundamental role in the activity of water erosion.
4. The study showed, by applying the Gavrilovic model, that the study area suffers from water erosion to a moderate degree.
5. The study area suffers from a fragile and highly sensitive environmental situation due to the nature of the extreme climate represented by the climate zone (BWH) according to the Köppen classification.

8. RECOMMENDATIONS

1- Embrace modern geographic technologies, such as Geographic Information Systems (GIS) and remote sensing, in hydrogeomorphological studies of water basins. Leveraging these technologies can lead to significant time, cost, and effort savings while delivering fast, precise results that closely align with real-world conditions relevant to the study.
2- Implement regular monitoring and surveillance measures in areas classified as highly eroded. Develop and implement appropriate erosion control and mitigation solutions tailored to the specific needs of these regions.
3- Advocate for the use of the Gavrilovic model among specialists and planners as a crucial step in the early stages of planning and development for any area. This model can provide valuable insights into erosion risks, enabling informed decision-making and sustainable development practices.
4- By adhering to these recommendations, it is possible to better manage and mitigate erosion issues in Ratka Valley basin and similar regions, leading to more sustainable land use and enhanced environmental protection.

REFERENCES

[1] Liu, B., Xie, Y., Li, Z., Liang, Y., Zhang, W., Fu, S., Guo, Q. (2020). The assessment of soil loss by water erosion in China. International Soil and Water Conservation Research, 8(4): 430-439. https://doi.org/10.1016/j.iswcr.2020.07.002

[2] Ghayeb, A.M., Mohammed, K.S. (2024). Surface runoff volume estimation for water harvesting in Al-Shagrah valley basin, western Anbar plateau. International Journal of Design & Nature and Ecodynamics, 19(3): 1089-1097. https://doi.org/10.18280/ijdne.190338

[3] Zhang, W., Zhou, J., Feng, G., Weindorf, D.C., Hu, G., Sheng, J. (2015). Characteristics of water erosion and conservation practice in arid regions of Central Asia: Xinjiang, China as an example. International Soil and Water Conservation Research, 3(2): 97-111. https://doi.org/10.1016/j.iswcr.2015.06.002

[4] Haregeweyn, N., Tsunekawa, A., Nyssen, J., Poesen, J., Tsubo, M., Tsegaye Meshesha, D., Tegegne, F. (2015). Soil erosion and conservation in Ethiopia: A review. Progress in Physical Geography, 39(6): 750-774. https://doi.org/10.1177/0309133315598725

[5] Buckhouse, J.C., Mattison, J.L. (1980). Potential soil erosion of selected habitat types in the high desert region of central Oregon. Rangeland Ecology & Management/Journal of Range Management Archives, 33(4): 282-285. https://doi.org/10.1016/S0140-1963(18)31560-X

[6] Lal, R. (1993). Soil erosion and conservation in West Africa. World Soil Erosion and Conservation, Cambridge Studies in Applied Ecology and Resource Management. Cambridge University Press, pp. 7-25.

[7] Chin, J.B., Takaijudin, H.B., Shafiai, S.H.B. (2022). Assessing downstream flood risk under changing climate for Bakun Dam in Sarawak. International Journal of Environmental Impacts, 5(4): 316-330. https://doi.org/10.2495/EI-V5-N4-316-330

[8] Du, H., Dou, S., Deng, X., Xue, X., Wang, T. (2016). Assessment of wind and water erosion risk in the watershed of the Ningxia-Inner Mongolia Reach of the Yellow River, China. Ecological Indicators, 67: 117-131. https://doi.org/10.1016/j.ecolind.2016.02.042

[9] Dunkerley, D.L., Brown, K.J. (1997). Desert soils. Arid zone geomorphology: Process, form and change in drylands, pp. 55-68.

[10] Breckle, S.W., Veste, M., Wucherer, W. (2001). Deserts, land use and desertification. In Sustainable Land Use in Deserts, pp. 3-13. Springer Berlin Heidelberg.

[11] Jeong, A., Dorn, R.I., Seong, Y.B., Yu, B.Y. (2021). Acceleration of soil erosion by different land uses in arid lands above ^{10}Be natural background rates: Case study in the Sonoran Desert, USA. Land, 10(8): 834. https://doi.org/10.3390/land10080834

[12] Farhan, Y., Nawaiseh, S. (2015). Spatial assessment of soil erosion risk using RUSLE and GIS techniques. Environmental Earth Sciences, 74: 4649-4669. https://doi.org/10.1007/s12665-015-4430-7

[13] Wainwright, J., Parsons, A.J., Abrahams, A.D. (1995). A simulation study of the role of raindrop erosion in the formation of desert pavements. Earth Surface Processes and Landforms, 20(3): 277-291. https://doi.org/10.1002/esp.3290200308

[14] Markose, V.J., Jayappa, K.S. (2016). Soil loss estimation and prioritization of sub-watersheds of Kali River basin, Karnataka, India, using RUSLE and GIS. Environmental Monitoring and Assessment, 188: 1-16. https://doi.org/10.1007/s10661-016-5218-2

[15] Ludwig, J.A., Muldavin, E., Blanche, K.R. (2000). Vegetation change and surface erosion in desert grasslands of Otero Mesa, southern New Mexico: 1982 to 1995. The American Midland Naturalist, 144(2): 273-285. https://doi.org/10.1674/0003-0031(2000)144[0273:VCASEI]2.0.CO;2

[16] Biswas, S.S., Pani, P. (2015). Estimation of soil erosion using RUSLE and GIS techniques: A case study of Barakar River basin, Jharkhand, India. Modeling Earth Systems and Environment, 1: 42. https://doi.org/10.1007/s40808-015-0040-3

[17] Akuja, T., Avni, Y., Zaady, E., Gutterman, Y. (2001). Soil erosion effects as indicators of desertification processes in the northern Negev Desert. In Soil Erosion, American Society of Agricultural and Biological Engineers. pp. 595-598. https://doi.org/10.13031/2013.4847

[18] Nearing, M.A., Simanton, J.R., Norton, L.D., Bulygin,

S.J., Stone, J. (1999). Soil erosion by surface water flow on a stony, semiarid hillslope. Earth Surface Processes and Landforms: The Journal of the British Geomorphological Research Group, 24(8): 677-686. https://doi.org/10.1002/(SICI)1096-9837(199908)24:8<677::AID-ESP981>3.0.CO;2-1

[19] Ozsoy, G., Aksoy, E., Dirim, M.S., Tumsavas, Z. (2012). Determination of soil erosion risk in the Mustafakemalpasa River Basin, Turkey, using the revised universal soil loss equation, geographic information system, and remote sensing. Environmental management, 50: 679-694.https://doi.org/10.1007/s00267-012-9904-8

[20] Rostagno, C.M., Degorgue, G. (2011). Desert pavements as indicators of soil erosion on aridic soils in north-east Patagonia (Argentina). Geomorphology, 134(3-4): 224-231. https://doi.org/10.1016/j.geomorph.2011.06.031

[21] Maltsev, K., Yermolaev, O. (2020). Assessment of soil loss by water erosion in small river basins in Russia. Catena, 195: 104726. https://doi.org/10.1016/j.catena.2020.104726

[22] Jiang, C., Zhang, H., Zhang, Z., Wang, D. (2019). Model-based assessment soil loss by wind and water erosion in China's Loess Plateau: Dynamic change, conservation effectiveness, and strategies for sustainable restoration. Global and Planetary Change, 172: 396-413. https://doi.org/10.1016/j.gloplacha.2018.11.002

[23] Papaiordanidis, S., Gitas, I.Z., Katagis, T. (2019). Soil erosion prediction using the Revised Universal Soil Loss Equation (RUSLE) in Google Earth Engine (GEE) cloud-based platform. Бюллетень Почвенного института им. ВВ Докучаева, 100: 36-52. https://doi.org/10.19047/0136-1694-2019-100-36-52

[24] Lane, L.J., Renard, K.G., Foster, G.R., Laflen, J.M. (1992). Development and application of modern soil erosion prediction technology-The USDA experience. Soil Research, 30(6): 893-912. https://doi.org/10.1071/SR9920893

[25] Poesen, J.W., Torri, D., Bunte, K. (1994). Effects of rock fragments on soil erosion by water at different spatial scales: A review. Catena, 23(1-2): 141-166. https://doi.org/10.1016/0341-8162(94)90058-2

[26] Gyssels, G., Poesen, J., Bochet, E., Li, Y. (2005). Impact of plant roots on the resistance of soils to erosion by water: A review. Progress in Physical Geography, 29(2): 189-217. https://doi.org/10.1191/0309133305pp443ra

[27] Almasalmeh, O., Saleh, A.A., Mourad, K.A. (2022). Soil erosion and sediment transport modelling using hydrological models and remote sensing techniques in Wadi Billi, Egypt. Modeling Earth Systems and Environment, 8(1): 1215-1226. https://doi.org/10.1007/s40808-021-01144-1

[28] Yang, J.L., Zhang, G.L., Yang, F., Yang, R.M., Yi, C., Li, D.C., Liu, F. (2016). Controlling effects of surface crusts on water infiltration in an arid desert area of Northwest China. Journal of Soils and Sediments, 16: 2408-2418. https://doi.org/10.1007/s11368-016-1436-z

[29] Wassif, M.M., Wassif, O.M. (2021). Sustainable soil management to mitigate soil erosion hazards in Egypt. In Management and Development of Agricultural and Natural Resources in Egypt's Desert, pp. 163-211. https://doi.org/10.1007/978-3-030-73161-8_7

[30] Mukanov, Y., Chen, Y., Baisholanov, S., Amanambu, A.C., Issanova, G., Abenova, A., Abayev, N. (2019). Estimation of annual average soil loss using the Revised Universal Soil Loss Equation (RUSLE) integrated in a Geographical Information System (GIS) of the Esil River basin (ERB), Kazakhstan. Acta Geophysica, 67: 921-938. https://doi.org/10.1007/s11600-019-00288-0

[31] Mohammad, K.S. Samat, N., Khalid, H.N. (2011). Using remote sensing and GIS for observation land use land cover changes and quantifying arable land loss in Penang Island-A case study of Balik Pulau. In 32nd Asian Conference on Remote Sensing 2011, ACRS 2011, 3: 1697-1715.